Magneto-optical effects in nanosandwich array with plasmonic structure of Au/[Co/Pt]$_n$/Au

Guan Xiang Du,[1,a)] Tetsuji Mori,[2] Michiaki Suzuki,[1] Shin Saito,[1] Hiroaki Fukuda,[2] and Migaku Takahashi[1]
[1]*Department of Electronic Engineering, Graduate School of Engineering, Tohoku University, 6-6-05 Aoba, Aramaki, Aoba-ku, Sendai 980-8579, Japan*
[2]*Device and Module Technology Development Center, Corporate Technology Development Group, Ricoh Company, Ltd., 16-1 Shinei-Cho, Tsuzuki-ku, Yokohama 224-0035, Japan*

(Presented 20 January 2010; received 29 October 2009; accepted 18 December 2009; published online 21 April 2010)

Nanodisk array with both sandwich structure of Au/[Co/Pt]$_n$/Au and [Co/Pt]$_n$ were fabricated by electron-beam lithography combined with ion milling process. Optical transmittance spectra revealed the excitation of localized surface plasmon resonance (LSPR) in Au/[Co/Pt]$_n$/Au nanosandwich array. Magneto-optical (MO) properties were measured by a micro-Faraday system with objective lens design and laser source. Faraday rotation angle for sandwich structure increased considerably compared to that of [Co/Pt]$_n$, indicating enhancement in MO activity by excitation of LSPR. The optical and MO properties of nanosandwich array were fitted in the framework of average field approximation. © *2010 American Institute of Physics*. [doi:10.1063/1.3368110]

Localized surface plasmon resonance (LSPR) is the collective electron charge oscillation that occurs in noble metal nanoparticles excited by light at the resonance frequency.[1] LSPR greatly enhances the localized electromagnetic field at metal/dielectric interfaces.[2] This phenomenon has been exploited in a variety of recent optical applications, including surface enhanced Raman scattering solar cells,[3] ultrasensitive bio/chemical sensors,[4] and light-emitting diodes.[5] Enhanced local fields give rise to enhanced light-matter interactions, which modify physical properties including light conversion efficiency,[3] florescence,[6] and magneto-optical (MO) properties. Incorporating MO materials into noble metal nanoparticles to produce composite MO materials has been demonstrated to artificially modify the spectral characteristics of MO activity. Despite nanosize confinement effects in MO materials having been intensively studied,[7,8] it was only recently recognized that LSPR can be utilized to further tailor MO properties by, for instance, using a noble-metal-coated core-shell structure[9] or a nanosandwich structure.[10] The spectral location of LSPR is sensitive to the size, shape, and arrangement of the nanoparticles, and also to the surrounding dielectrics. These factors provide considerable freedom to tune the MO spectral characteristics, but it remains unclear how they affect the MO properties. Compared to chemical methods[9] or nanosphere lithography,[10] nanofabrication by a combination of electron-beam lithography (EBL) and ion milling provides easier control of the size, shape, and arrangement of nanostructures as well as a narrower nanoparticle size distribution.

In this study, square nanodisk arrays with multilayer structures ([Co/Pt]$_n$) and with sandwich structures (Au/[Co/Pt]$_n$/Au) were fabricated by EBL combined with argon-ion milling. The grating constant was 250 nm and the disk diameter was varied in the range 50–130 nm. Thin films with structures of Ti(2)/Pt(1)/[Co(0.5)/Pt(1)]$_7$/Pt(3) and Ti(2)/Au(20)/Pt(1)/[Co(0.5)/Pt(1)]$_7$/Au(20) (in nanometers) were grown by sputtering on glass substrates with a Ti buffer layer; hereafter, these structures are denoted by [Co/Pt]$_n$ and Au/[Co/Pt]$_n$/Au, respectively. The Faraday rotation angle and the ellipticity of each disk array were measured using a homemade micro-Faraday system with an objective lens design and a laser light source. A magnetic field was applied parallel to the light beam and perpendicular to the sample plane. The chip had dimensions of 150 $\times$ 150 μm^2 and was larger than the light spot. The optical and MO properties of the nanosandwich array were simulated in the framework of average field approximation (AFA) following Abe's method.[11]

The negative resist of TGMR (from TOK) was used for the mask in EBL, which was performed using a JBX-5000SD (JOEL). The resist thickness was in the range of 100–150 nm, which is appropriate for pattern transfer in ion milling. A writing current of −8.5 pA and a dosage in the range of 27–60 μC/μm^2 were adopted to fabricate small disks. Figure 1(a) shows an SEM image of the resist mask for a nanodisk array with a disk diameter (d) of 84 nm and a grating constant (h) of 250 nm (the same value of h was used throughout this study). The double-ended arrow in Fig. 1(a) indicates the polarization direction of the incident light for both optical and MO measurements. Argon-ion milling was performed at a small tilt angle of 10° to transfer the resist mask pattern. Finally, the nanodisk was spin coated to produce a 150-nm-thick resist layer. In the following discussion, the disk size is taken to be that of the resist mask, even though its actual size might differ from the measured one due to redeposition. The permittivities of a continuous gold film and a [Co(0.5)/Pt(1)]$_m$ (m=30) multilayer structure was measured using an ellipsometer, as shown in Fig. 1(b); the

a)Author to whom correspondence should be addressed. Electronic mail: gxdu@ecei.tohoku.ac.jp.

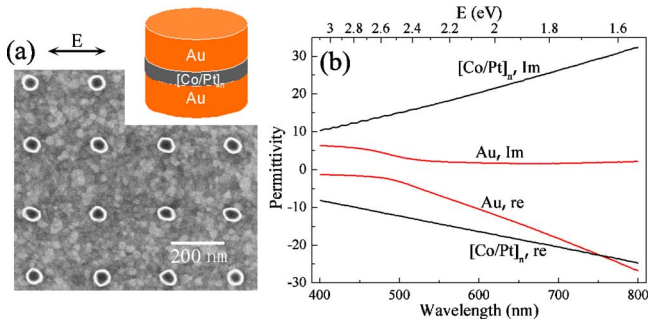

FIG. 1. (Color online) (a) SEM image of nanodisk array and schematic view of nanosandwich consisting of Au/$[Co/Pt]_n$/Au, double-ended arrow shows the relative polarization of light with respect to the array at normal incidence. (b) Permittivity of Gold continuous film and $[Co(0.5)/Pt(1)]_n$ multilayer for wavelength of 400–800 nm.

permittivity of gold film has a much smaller imaginary component than that of $[Co/Pt]_n$.

Transmission spectra of the nanosandwich array with a structure of Au/$[Co/Pt]_n$/Au was measured by a microspectrometer with a small numerical aperture of 0.13 in the wavelength range of 400–800 nm. Due to the large optical extinction cross-section associated with LSPR, transmittance spectra exhibit a minimum at the resonance wavelength. Figure 2(a) shows transmittance spectra for Au(40), $[Co(0.5)/Pt(1)]_7$, and Au(20)/$[Co(0.5)/Pt(1)]_7$/Au(20) (unit: nanometers) with approximately the same diameters (d=108 nm). The transmittance minimum at around 700 nm indicates that LSPR was excited in both the gold nanodisk array and the nanosandwich array, whereas the spectrum of $[Co/Pt]_7$ is featureless. By varying the disk diameter, LSPR could be excited in both structures and it was redshifted when the disk size was increased (not shown). The LSPR spectrum of the nanodisk array with a sandwich structure is similar to that of gold, while the peak is broadened due to the insertion of a dispersive material $[Co/Pt]_7$. To understand the transmittance spectra of the nanodisk array, all the local and far-field components of the nanodisks acting on each other and on the dielectric background should be considered. For simplicity, we treat it using the free nanoparticle approximation in

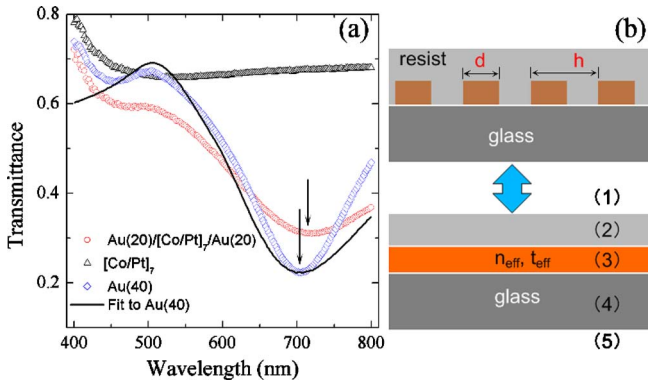

FIG. 2. (Color online) (a) Transmittance spectra of $[Co/Pt]_7$, Au, and Au/$[Co/Pt]_7$/Au nanodisk array with the same size d of 108 nm. LSPR was excited for both Au and Au/$[Co/Pt]_n$/Au indicated by arrows. Solid line shows the fitted data for gold nanodisk array. (b) Illustration diagram of the fitting model in which nanodisk array was approximated by a slab with effective refractive index n_{eff} and thickness t_{eff}.

which all the particles are identical and the local fields both inside and outside the particle are averaged; this is the basic concept of AFA.[11] In this study, the nanodisk array was approximated by a slab with an effective thickness and permittivity. As shown in Fig. 2(b), the gold nanodisk array (d,h) is replaced by an effective slab (3) with an effective refractive index ($n_3=n_{\text{eff}}$) and thickness (t_{eff}). Light propagates through (1)–(5); the refractive indices for layers (1–5) are 1, 1.5, n_{eff}, 1.5, and 1, respectively, and t_{eff} of the slab is assumed to be equal to t_{Au} (40 nm). The effective permittivity (ε_{eff}) was deduced in the AFA framework.[12] The transmittance spectra for the gold nanodisk array are fitted (the MO properties of the nanosandwich array are discussed below). The transmittance (T) and transmission coefficient (t) are given by:

$$T=|t|^2,\quad t=t_{12}t_{23}t_{34}t_{45}e^{i\delta_3}, \tag{1}$$

where

$$t_{ij}=2n_i/(n_i+n_j),$$

$$\delta_3=2\pi n_{\text{eff}}t_{\text{eff}}/\lambda,$$

$$n_{\text{eff}}=\sqrt{\varepsilon_{\text{eff}}}, \tag{2}$$

and

$$\varepsilon_{\text{eff}}=(1-g)\varepsilon_d+g\varepsilon_{\text{Au}},$$

$$g=f/A,$$

$$A=1+(1-f)N(\varepsilon_{\text{Au}}-\varepsilon_d)/\varepsilon_d. \tag{3}$$

Equation (1) does not consider multiple reflections since the nanodisk array is not a real slab with smooth surfaces. f is the volume fraction of nanodisk in the slab, ε_{Au} is the permittivity of gold, and ε_d is the permittivity of the surrounding resist. The fitting results indicate that the quantity ε_d should be treated as a fitting parameter rather than the intrinsic permittivity of the resist (2.25) to account for the polarization effect of the electric field of the nanodisk array acting on the surrounding resist. The depolarization factor (N) is a complex number; its real part is determined by the shape and was calculated by modeling the nanodisks as oblate spheroids,[12] while its imaginary part is a fitting parameter, which was found to have a small magnitude and is attributed to radiation effects.[13] For a gold nanodisk array with d =108 nm and h=250 nm, these two fitting parameters are ε_d=4.0 and N=0.1958−0.057i. The fitting results shown in Fig. 2(a) are in good agreement with the experimental data, indicating that AFA captures the main features. For disk sizes in the range $50<d<120$ nm, the imaginary part of N varies between −0.06 and −0.05 and $\varepsilon_d \in (3.9,4.8)$. All the fitting results exhibit good consistency.

The MO properties of the nanosandwich array were measured and compared with those of the $[Co/Pt]_7$ nanodisk array. The light source was a He–Ne laser (633 nm) with the polarization in the direction shown in Fig. 1(a). The Faraday rotation angle and ellipticity loops were obtained. The MO properties were obtained by subtracting the contribution of the glass substrate and they are summarized in Figs. 3(a) and 3(b). The absolute value of the rotation angle was remark-

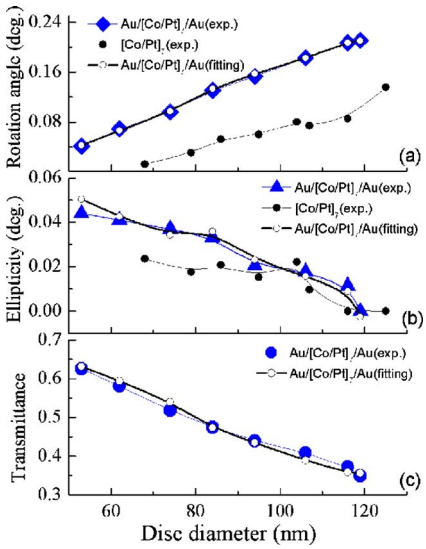

FIG. 3. (Color online) (a) Rotation angle, (b) ellipticity, and (c) transmittance of nanosandwich array as a function of disk diameter at 633 nm, both experimental and fitting data are shown in each panel. Rotation angle and ellipticity of $[Co/Pt]_n$ nanodisk array are shown in (a) and (b), respectively, for comparison.

ably higher in the sandwich structure; for example, it was 0.085° for the $[Co/Pt]_7$ nanodisk array with a disk size d of 116 nm, while it was 0.207° for the nanosandwich array with the same disk size (i.e., a factor of 2.4 higher). This result indicates that MO activity was enhanced by LSPR by the incorporation of gold. To simulate the MO properties in AFA, the sandwich structure was assumed to be a homogeneous material with a bulk permittivity tensor. By considering the volume fraction factor of $[Co/Pt]_7$ in the sandwich structure, the diagonal of the bulk permittivity tensor is given by $\varepsilon_{xx}^{san}=-14.8+6.7i$, which is the volume-averaged value of Au and that of $[Co/Pt]_7$ ($\varepsilon_{Au}=-12.885+1.638i, \varepsilon_{Co/Pt}=-20.700+21.832i$); the off-diagonal part is chosen to be 1/5 of that of $[Co/Pt]_n$, which is $\varepsilon_{xy}^{san}=(0.3173-0.0207i)/5$ measured for $[Co(0.5)/Pt(1)]_n$ in the polar Kerr configuration at $\lambda=633$ nm. The effective permittivity tensor of the slab has diagonal and off-diagonal components given by

$$\varepsilon_{xx}^{eff}=(1-g_2)\varepsilon_{d2}+g_2\varepsilon_{xx}^{san},$$

$$\varepsilon_{xy}^{eff}=h_2\varepsilon_{xy}^{san} \quad (4)$$

where

$$g_2=f_2/A_2,$$

$$h_2=f_2/A_2^2,$$

$$A_2=1+(1-f_2)N_2(\varepsilon_{xx}^{san}-\varepsilon_{d2})/\varepsilon_{d2} \quad (5)$$

The transmittance was calculated using Eqs. (1) and (2) by replacing n_{eff} with n_{eff2}

$$n_{eff2}=\sqrt{\varepsilon_{xx}^{eff}}. \quad (6)$$

The Faraday rotation angle θ_F and the ellipticity η_F are given by[14]

$$\theta_F-i\eta_F=i\pi t_{eff2}\varepsilon_{xy}^{eff}/(\lambda n_{eff2}). \quad (7)$$

The effective thickness is $t_{eff2}=t_{Au}+t_{[Co/Pt]}$. f_2 is the volume fraction of the nanosandwich in the slab. The two fitting parameters are the complex depolarization factor N_2 and the permittivity of the resist ε_{d2}. As shown in Fig. 3, good agreement was obtained between the experimental data and the fitted data in terms of the rotation angle, the ellipticity, and the transmittance.

In summary, nanodisk arrays with a sandwich structure of $Au/[Co/Pt]_n/Au$ and with a $[Co/Pt]_n$ multilayer structure were fabricated by EBL and argon-ion milling, which enable the size, shape, and arrangement of nanostructures to be easily controlled so that the spectra location of LSPR can be tuned. The optical and MO properties of both structures were investigated over a range of disk sizes. The results reveal that the nanosize effect modifies the MO spectral characteristics. Moreover, the rotation angle of the sandwich structure is considerably higher than that of $[Co/Pt]_n$, indicating enhancement in MO activity by excitation of LSPR associated with gold in the sandwich structure. Transmittance spectra of the gold nanodisk array and the optical and MO properties of the nanosandwich array were fitted in the AFA framework.

ACKNOWLEDGMENTS

This work was partly supported by JSPS program of Postdoctoral Fellowship for Foreign researchers (Grant-in-Aid No. 2109282).

[1] E. Hutter and J. H. Fendler, Adv. Mater. **16**, 1685 (2004).
[2] E. Hao and G. C. Schatz, J. Chem. Phys. **120**, 357 (2004).
[3] C. Hägglund, M. Zäch, G. Petersson, and B. Kasemo, Appl. Phys. Lett. **92**, 053110 (2008).
[4] J. N. Anker, W. P. Hall, O. Lyandres, N. C. Shah, J. Zhao, and R. P. Van Duyne, Nature Mater. **7**, 442 (2008).
[5] J. H. Sung, B. S. Kim, C. H. Choi, M. W. Lee, S. G. Lee, S. G. Park, E. H. Lee, and O. B. Hoan, Microelectron. Eng. **86**, 1120 (2009).
[6] Y. Chen, K. Munechika, I. J. Plante, A. M. Munro, S. E. Skrabalak, Y. Xia, and D. S. Gingera, Appl. Phys. Lett. **93**, 053106 (2008).
[7] J. L. Menéndez, B. Bescós, G. Armelles, R. Serna, J. Gonzalo, R. Doole, A. K. Petford-Long, and M. I. Alonso, Phys. Rev. B **65**, 205413 (2002).
[8] V. G. Kravets, A. K. Petford-Long, and A. F. Kravets, J. Appl. Phys. **87**, 1762 (2000).
[9] P. K. Jain, Y. Xiao, R. Walsworth, and A. E. Cohen, Nano Lett. **9**, 1644 (2009).
[10] J. B. González-Díaz, A. García-Martín, J. M. García-Martín, A. Cebollada, G. Armellel, B. Sepúlveda, Y. Alaverdyan, and M. Käll, Small **4**, 202 (2008).
[11] M. Abe, Phys. Rev. B **53**, 7065 (1996).
[12] J. Venermo and A. Sihvola, J. Electrostat. **63**, 101 (2005).
[13] T. Jensen, L. Keely, A. Lazarides, and G. Schatz, J. Cluster Sci. **10**, 295 (1999).
[14] S. Sugano and N. Kojima, *Magneto-Optics* (Springer, New York, 2000), p. 143.